

The Reaction $pp \rightarrow p + X$ at 405 GeV/c.*

A. A. Seidl

The University of Michigan, Ann Arbor, Michigan 48104

ABSTRACT

Preliminary results on the reaction $pp \rightarrow p + X$ from an exposure of the NAL 30 inch liquid hydrogen bubble chamber are presented. Single particle inclusive distributions are discussed and compared with corresponding data at 102 GeV/c.

INTRODUCTION

I would like to present some preliminary results on the reaction $pp \rightarrow p + X$ at a beam momentum of 405 GeV/c. Table I lists the physicists contributing to this as well as to the similar experiment at 102 GeV/c.

Table I List of Contributing Physicists

<u>University of Rochester</u>	<u>University of Michigan</u>
C. Bromberg	J. Chapman
D. Cohen	J. Cooper
T. Ferbel	N. Green
P. Slattery	B. Roe
	A. Seidl
	J. VanderVelde

DISCUSSION

We have identified events belonging to the reaction $pp \rightarrow p + X$ by the requirement that the observed ionization of the proton be consistent with its measured momentum. In order to insure a clean separation between p's and π 's and K's we have used only protons whose laboratory momentum is less than 1.2 GeV/c. Due to the rapid fall off of the data as a function of the transverse momentum (the data when fitted to an exponential in p_T^2 have a slope of $\sim 7.5 \text{ GeV}^{-2}$) the requirement that the laboratory momentum of the proton be less than 1.2 GeV/c does not bias distributions in $x = 2p_L^*/\sqrt{s}$ for $x < 0.5$. The variables p_L^* and \sqrt{s} are respectively the longitudinal momentum and the energy in the center of the mass.

In order to separate elastically scattered protons from protons produced by inelastic reactions, we have fitted all two prongs to the four constraint reaction $pp \rightarrow pp$. Since we cannot reliably measure the magnitude of the momentum of the fast tracks in the

30 inch bubble chamber, we have used the nominal beam momentum, 405 GeV/c, for both the beam track and the fast outgoing track with errors of ± 1 GeV/c on both. This effectively reduces the fits to two constraints. However we feel that the fit is an effective way of reducing the amount of elastic contamination in the inelastic sample.

In Figure 1a(1b) we plot $d\sigma/dx$ ($d\sigma/dM^2$) for the inclusive reaction $pp \rightarrow p + X$. Except in the vicinity of $x = 0$, the mass squared recoiling against the observed proton is related to the x of the proton by $M^2 \approx m_p^2 + s(1+x)$, where m_p is the proton's mass. The data at 405 GeV/c are plotted as circles and, for comparison, the superimposed histograms are the data from 102 GeV/c.

The data displayed in Figure 1a, $d\sigma/dx$, exhibit two main features. First of all the data at 405 and 102 GeV/c scale (to within the statistical accuracy of the data) for $x > -0.9$. Secondly the peak in the cross section near $x = -1$ increases in size and narrows (so as to maintain approximately the same area) as the lab momentum increases from 102 to 405 GeV/c. The increase in the cross section at $x \approx -1$ is reflected in the approximate constancy of $d\sigma/dM^2$, Figure 1b, for small values of M^2 . In fact, on closer inspection, there appear to be three regions of variables with different scaling properties: the region $x \gtrsim -0.9$ in which $d\sigma/dx$ scales,

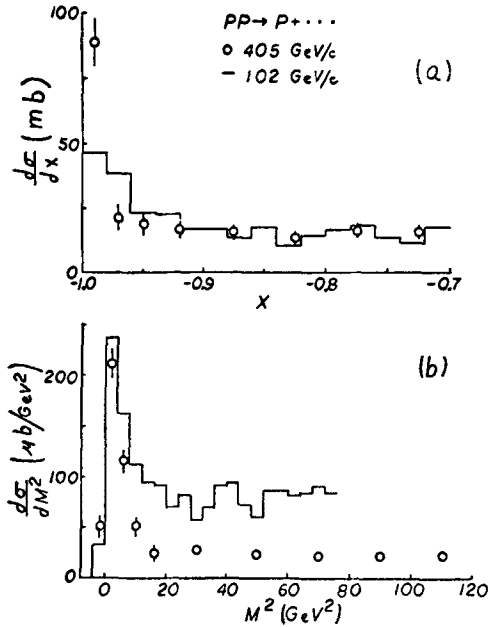


Fig.1. Inclusive distributions of a) $d\sigma/dx$ and b) $d\sigma/dM^2$.

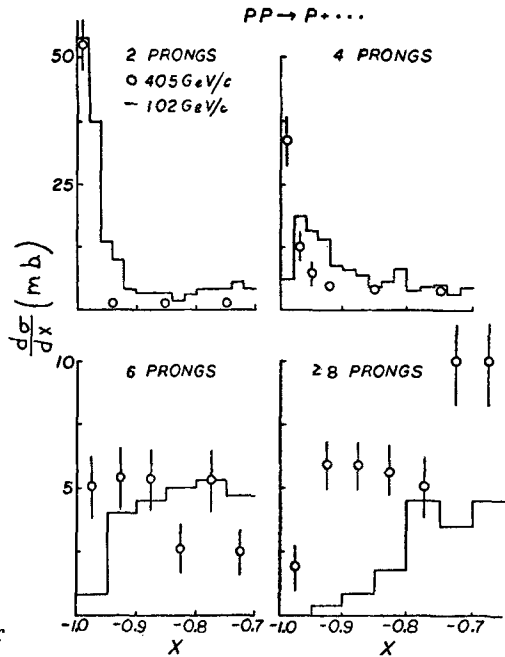


Fig. 2. Distributions of $d\sigma/dx$ versus charged prong multiplicity.

the region $M^2 \lesssim 10 \text{ GeV}^2$ in which $d\sigma/dM^2$ scales, and an intermediate region in which both $d\sigma/dx$ and $d\sigma/dM^2$ fall with increasing s .

To illustrate that any possible elastic contamination does not effect these conclusions and to illustrate how the various topologies build up the inclusive cross section, we plot in Figures 2 and 3

$d\sigma/dx$ and $d\sigma/dM^2$ for various charged topologies. The peak for small M^2 ($x \approx -1$) comes mainly from the two and four prong topologies indicating that the major diffractive contribution is to low multiplicities. There is also some indication (although this could be affected by elastic contamination) that the two prong distributions are somewhat narrower than the four prong distributions.

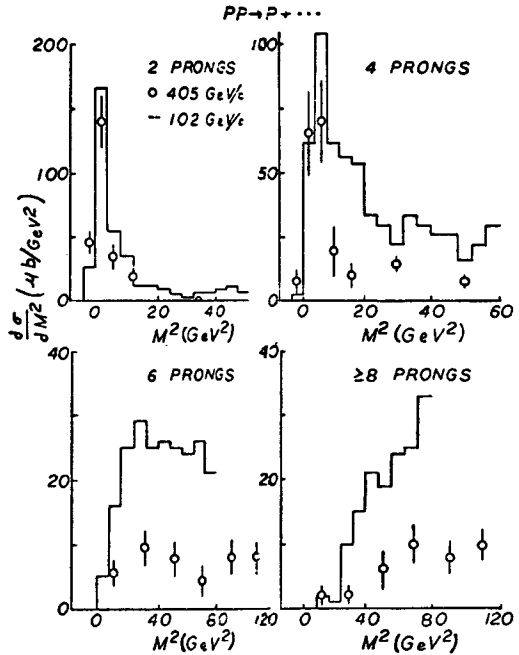


Fig.3. Distributions of $d\sigma/dM^2$ versus charged prong multiplicity.

CONCLUSION

We have observed evidence that there may be three distinct regions of variables with different scaling properties in the study of the reaction $pp \rightarrow p + X$: $x > -0.9$ where $d\sigma/dx$ scales, $M^2 < 10 \text{ GeV}^2$ where $d\sigma/dM^2$ approximately scales, and the intermediate region in which both $d\sigma/dx$ and $d\sigma/dM^2$ decrease with increasing s .